Supporting Information

Sulfur Doping Enhanced Desorption of Intermediates on NiCoP for Efficient Alkaline Hydrogen Evolution

*Yuyang Qi,[1] Long Zhang,[2] Lan Sun,[1] Guanjun Chen,[1] Qiaomei Luo,[1] Hongqiang Xin,[1] Jiahui Peng,[2] Yan Li [*1] and Fei Ma [*1]*

[1]State Key Laboratory for Mechanical Behavior of Materials, Xi'an Jiaotong University, Xi'an 710049, Shaanxi, China

[2] School of Materials Science and Engineering, Chang'an University, Xi'an 710061, China

Materials:

Sodium hypophosphite ($NaH_2PO_2 \cdot H_2O$), nickel nitrate hexahydrate ($Ni(NO_3)_2 \cdot 6H_2O$) and sulfur were purchased from Sinopharm Chemical Reagent Co., Ltd. (Shanghai, China). Cobalt nitrate hexahydrate ($Co(NO_3)_2 \cdot 6H_2O$) and urea ($CO(NH_2)_2$) were bought from Macklin Biochemical Co., Ltd. (Shanghai, China). CFP was purchased from He Sen Corporation (type: TGP-H-060). All the reagents were used as received.

Turnover Frequency Calculations.

The size of electrochemical active surface area (A_{ECSA}) can be calculated using the following formula[1, 2]:

$$A_{ECSA} = \frac{C_{dl-catalyst}(mF \cdot cm^{-2})}{C_{dl-CFP}(mF \cdot cm^{-2})\ per\ cm^2_{ECSA}} \quad (1)$$

The specific capacitance of CFP is normally treated as 0.04mF·cm^{-2}.

Turnover frequency (TOF) is calculated from the following formula:

$$TOF = \frac{number\ of\ total\ H_2\ turnovers\ /\ geometric\ area(cm^2)}{number\ of\ surface\ active\ sites\ /\ geometric\ area(cm^2)} \quad (2)$$

The number of total H_2 turnover can be calculated from the current density (j) according to:

$$No.\ of\ H_2 = \left(|j|\frac{mA}{cm^2}\right)\left(\frac{1\ Cs^{-1}}{1000mA}\right)\left(\frac{1\ mol\ e^-}{96485.3\ C}\right)\left(\frac{1\ mol\ H_2}{2\ mol\ e^-}\right)\left(\frac{6.022\times10^{23}\ H_2\ molecules}{1\ mol\ H_2}\right)$$
$$= 3.12\times10^{15}\ \frac{H_2/s}{cm^2}\ per\ \frac{mA}{cm^2} \quad (3)$$

Since the nature of the surface active sites is not yet clarified and the exact hydrogen binding site is not known, we estimate the number of active sites as the total number of surface sites (including both Ni, Co, P and S atoms as possible active sites) from the unit cell of the catalysts, which may underestimate the real TOF.

The active sites per real surface area is calculated from the following formula:

$$No.\ of\ active\ sites = \left(\frac{No.\ of atoms / unit\ cell}{Volume / unit\ cell} \right)^{\frac{2}{3}} \quad (4)$$

We can calculate the number of active sites per real surface area for each phase. The exact cell parameters of $Ni_{1.5}Co_{1.5}S_4$ is from the average value of $NiCo_2S_4$ and $CoNi_2S_4$.

$$No.\ of\ active\ sites(NiCoP) = (\frac{9\ atoms / unit\ cell}{98.77\ \text{Å}/\ unit\ cell})^{\frac{2}{3}} = 2.02 \times 10^{15}\ atoms\ cm^2 \quad (5)$$

$$No.\ of\ active\ sites(Ni_{1.5}Co_{1.5}S_4) = (\frac{14\ atoms / unit\ cell}{825.56\ \text{Å}/\ unit\ cell})^{\frac{2}{3}} = 6.60 \times 10^{14}\ atoms\ cm^2$$

(6)

Finally, the TOF can be calculated from the following formula:

$$TOF = \frac{\left(3.12 \times 10^{15} \frac{H_2 / s}{cm^2}\ per\ \frac{mA}{cm^2} \right) \times |j|}{No.\ of\ active\ sites \times A_{ECSA}} \quad (7)$$

The formation of precursor NWs.

The precursor is a template as a nanowire array. Its formation can be expressed by the following chemical reaction equation：

$$H_2NCONH_2 + H_2O \rightarrow 2NH_3 + CO_2 \quad (8)$$

$$CO_2 + H_2O \rightarrow CO_3^{2-} + 2H^+ \quad (9)$$

$$Co^{2+} + 0.5(2-x)CO_3^{2-} + xOH^- + nH_2O \rightarrow Co(OH)_x(CO_3)_{0.5(2-x)} \cdot nH_2O \quad (10)$$

The doping of Ni replaces the position of Co in the unit cell without changing the phase. The speed of crystal growth is controlled by the process conditions to grow along the surface with the highest energy to form single crystal nanowires, and a uniform ordered nano-array is formed on the surface of the carbon fiber.

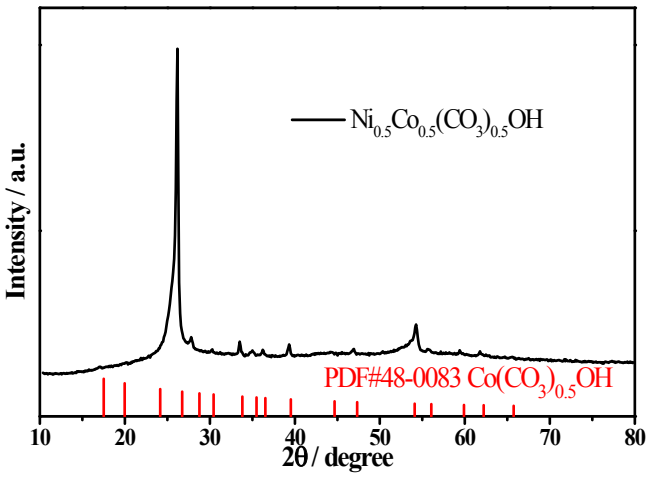

Figure S1. XRD of the precursor.

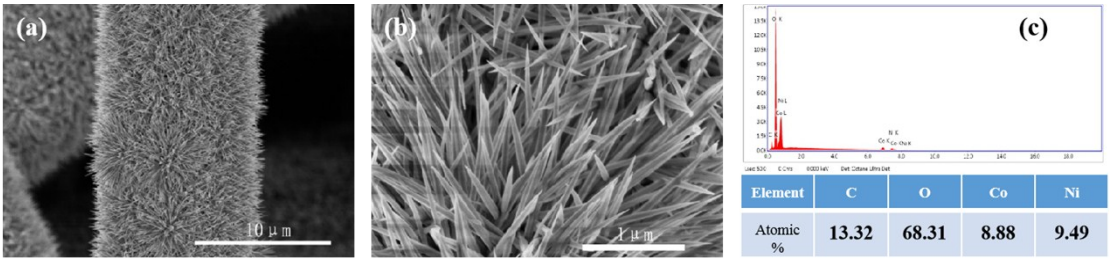

Element	C	O	Co	Ni
Atomic %	13.32	68.31	8.88	9.49

Figure S2. (a,b) SEM, (c) EDS of the precursor.

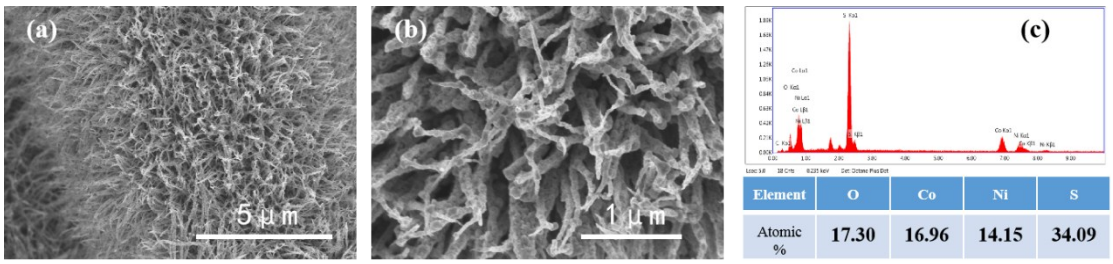

Element	O	Co	Ni	S
Atomic %	17.30	16.96	14.15	34.09

Figure S3. (a,b) SEM, (c) EDS of NiCo-sulfide NWs

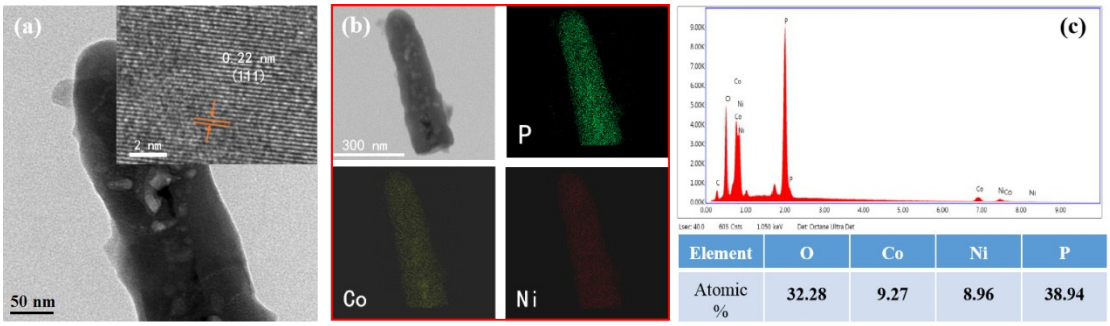

Element	O	Co	Ni	P
Atomic %	32.28	9.27	8.96	38.94

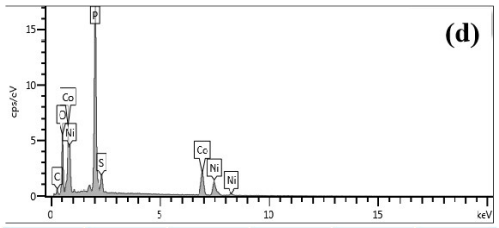

Element	O	Co	Ni	P	S
Atomic %	25.66	15.3	11.92	28.1	3.07

Figure S4. (a) TEM image, (b) EDS elemental mapping, (c) EDS of NiCoP NWs, (d) EDS of S-NiCoP NWs. Inset in (a): HRTEM image of NiCoP NWs.

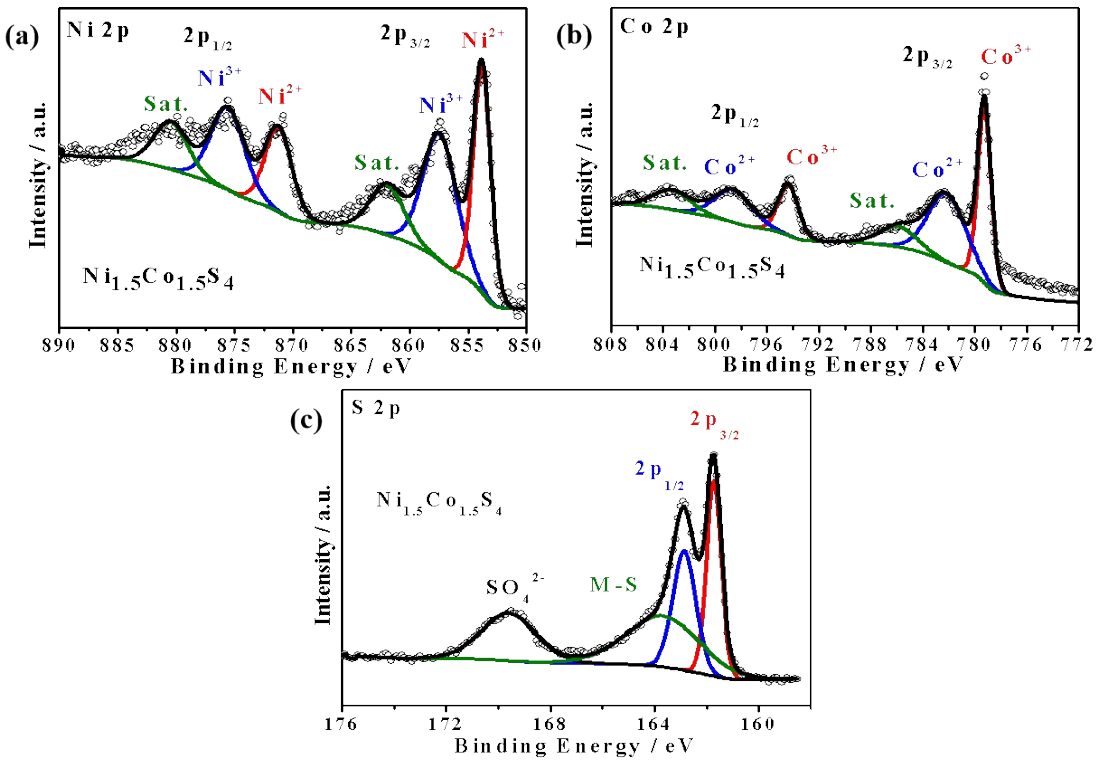

Figure S5. XPS of (a) Ni 2p, (b) Co 2p and (c) S 2p of $Ni_{1.5}Co_{1.5}S_4$.

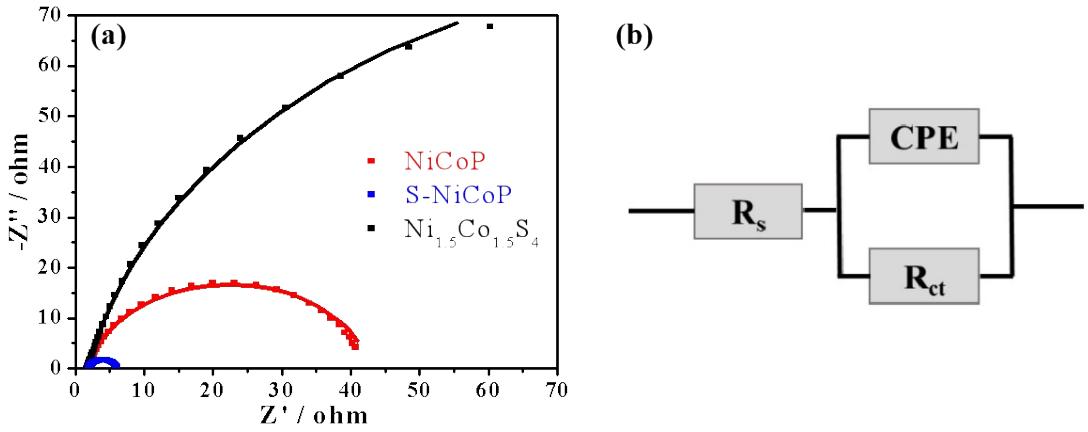

Figure S6. (a) EIS Nyquist plots and (b) The equivalent circuit.

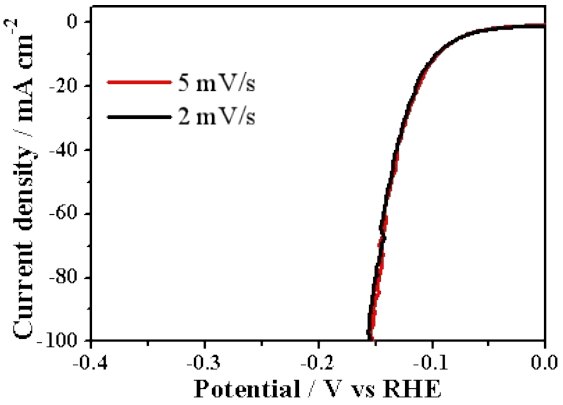

Figure S7. Linear sweeping voltammetry of S-NiCoP NWs at different scan rate. The HER performance of the sample is hardly affected by the scan rate.

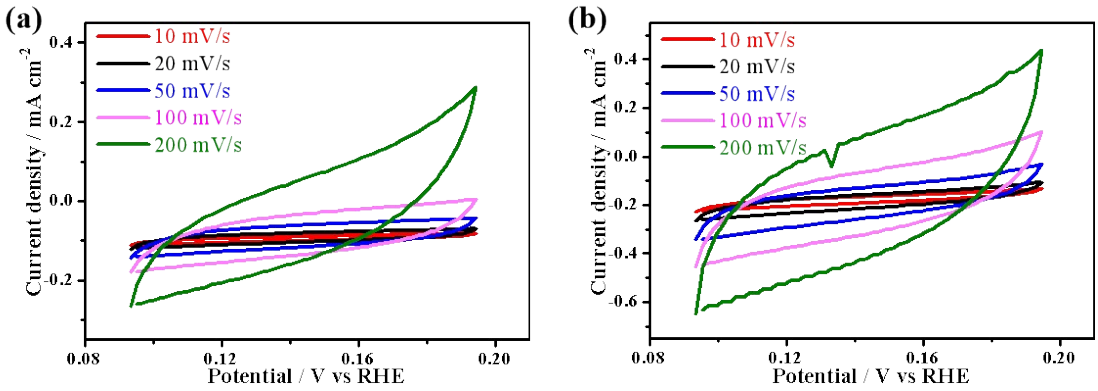

Figure S8. Electrochemical double-layer capacitance measurements of (a) NiCoP and (b) S-NiCoP.

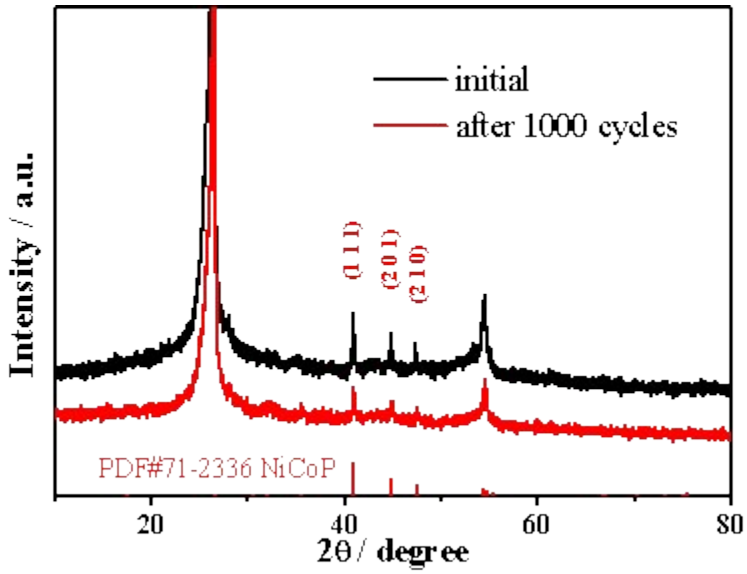

Figure S9. XRD of S-NiCoP NWs before and after 1000 cycles.

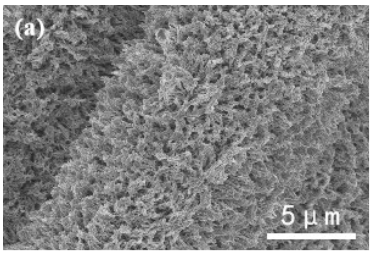

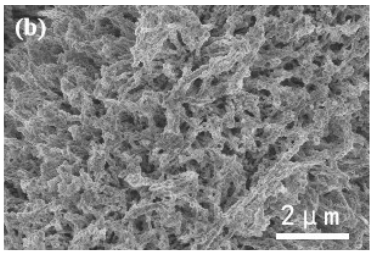

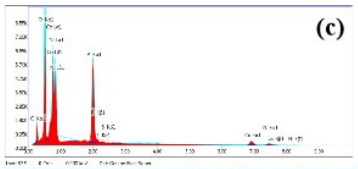

Element	O	Co	Ni	P	S
Atomic %	35.92	10.11	10.22	22.93	1.87

Figure S10. (a,b) SEM, (c) EDS of S-NiCoP NWs after 1000 cycles.

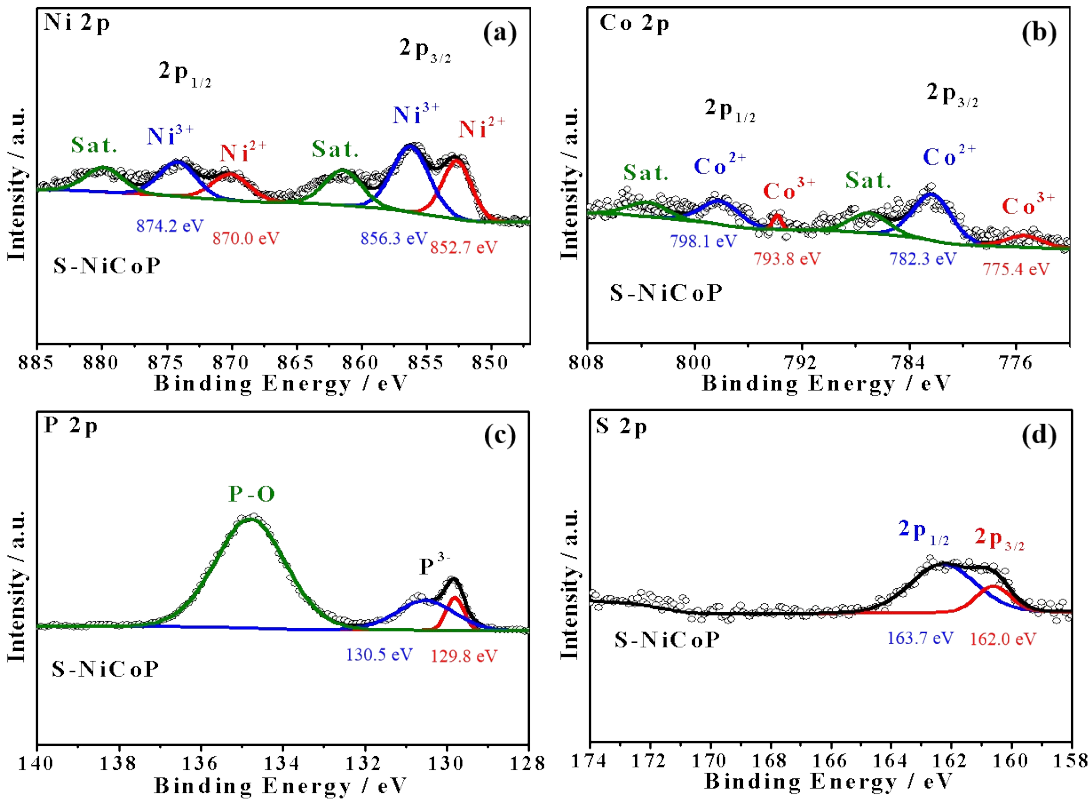

Figure S11. XPS of (a) Ni 2p, (b) Co 2p, (c) P 2p and (d) S 2p of S-NiCoP NWs after 1000 cycles.

As shown in Figures S12-S15, the content of S could be fine adjusted through reducing the content of P source and shortening the phosphorization time. The obtained samples were named according to the P/S ratio (from EDS in Figure S4, S12 and S13). If only a small amount of S atoms are doped (NiCo-$P_{0.90}S_{0.10}$ and NiCo-$P_{0.77}S_{0.23}$), the samples will maintain the structure of nanowires (Figure 1e,f and Figure S12a) and the main phase of NiCoP (Figure 1b and Figure S14a). However, if a larger amount of S atoms are doped (NiCo-$P_{0.45}S_{0.55}$), micro-flakes appeared (Figure S13a) with new phases of CoPS and $NiCo_2S_4$ (Figure S14b).

As shown in Figure S15a, the η_{100} values of NiCo-$P_{0.90}S_{0.10}$ and NiCo-$P_{0.77}S_{0.23}$ are lowered from 260 mV of pure NiCo-P down to 172 mV and 245 mV, respectively, but that of NiCo-$P_{0.45}S_{0.55}$ is increased up to 337 mV. It indicates that a small amount of S doping (NiCo-$P_{0.90}S_{0.10}$ and NiCo-$P_{0.77}S_{0.23}$) could regulate the electronic states and improve the HER performances of NiCoP, although the morphology and phase are maintained. NiCo-$P_{0.90}S_{0.10}$ exhibits the best HER performance. As for NiCo-$P_{0.45}S_{0.55}$ with larger amount of S dopants, the HER activity is lowered due to the changed morphology and phase transition. The Tafel slope (Figure S15b) of NiCo-$P_{0.90}S_{0.10}$ (63.3 mV·dec^{-1}) is also the smallest one, that is, an appropriate S doping could promote the electron transfer during the Heyrovsky reaction and increase the HER activity.

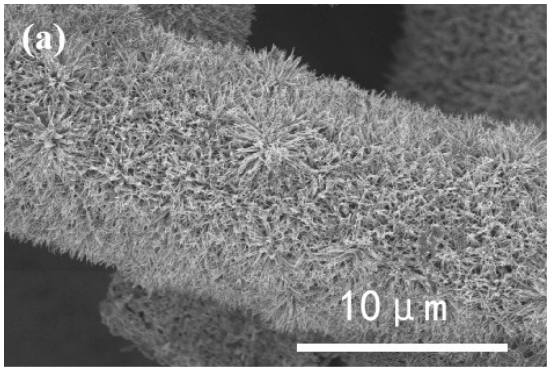

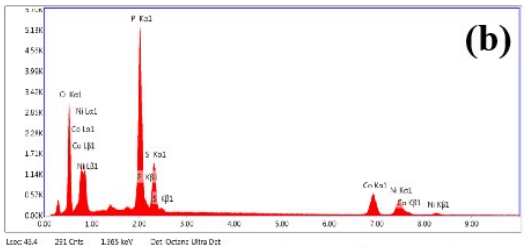

Element	O	Co	Ni	P	S
Atomic %	41.23	13.33	11.91	25.93	7.6

Figure S12. (a) SEM, (b) EDS of NiCo-$P_{0.77}S_{0.23}$ NWs.

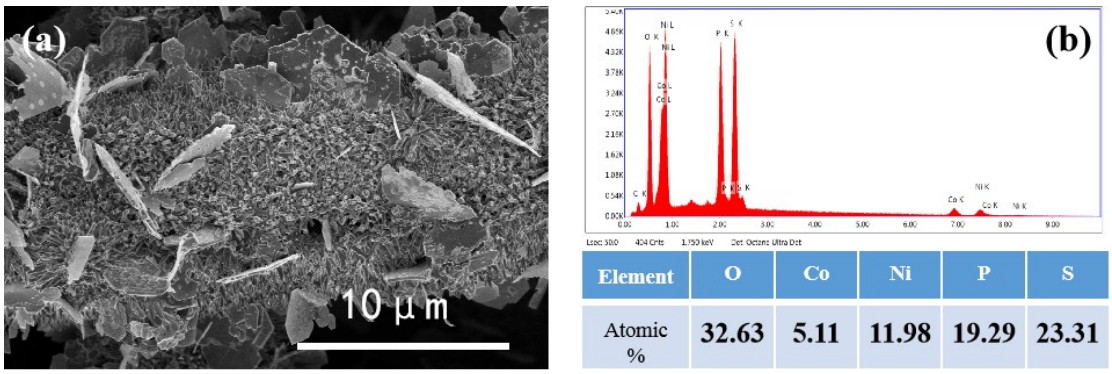

Element	O	Co	Ni	P	S
Atomic %	32.63	5.11	11.98	19.29	23.31

Figure S13. (a) SEM, (b) EDS of NiCo-$P_{0.45}S_{0.55}$ NWs.

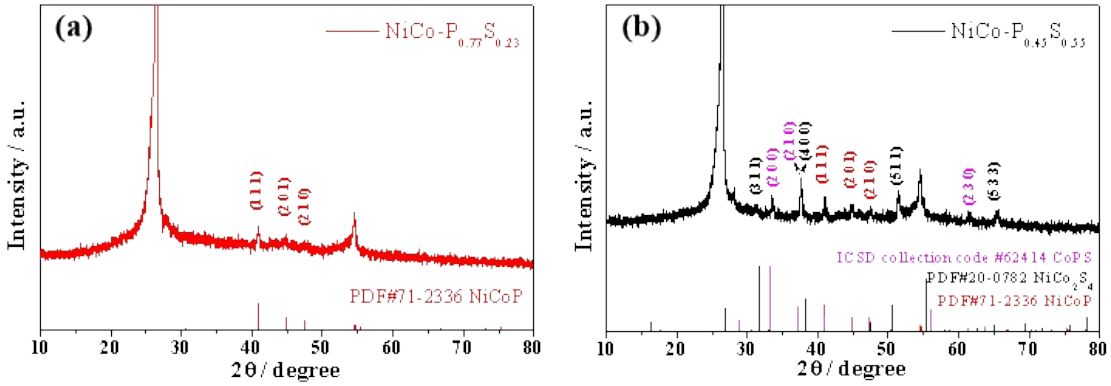

Figure S14. XRD of (a) NiCo-$P_{0.77}S_{0.23}$ NWs and (b) NiCo-$P_{0.45}S_{0.55}$ NWs. The phase CoPS is from literature[3].

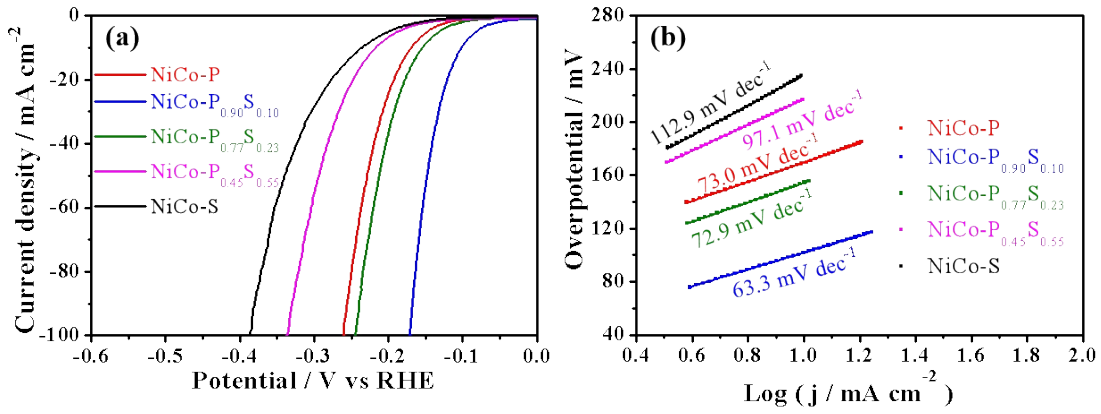

Figure S15. (a) Linear sweeping voltammetry, (b) Tafel plots for different content of sulfur. NiCo-P, NiCo-$P_{0.90}S_{0.10}$ and NiCo-S denote NiCoP, S- NiCoP and $Ni_{1.5}Co_{1.5}S_4$ in this paper, respectively.

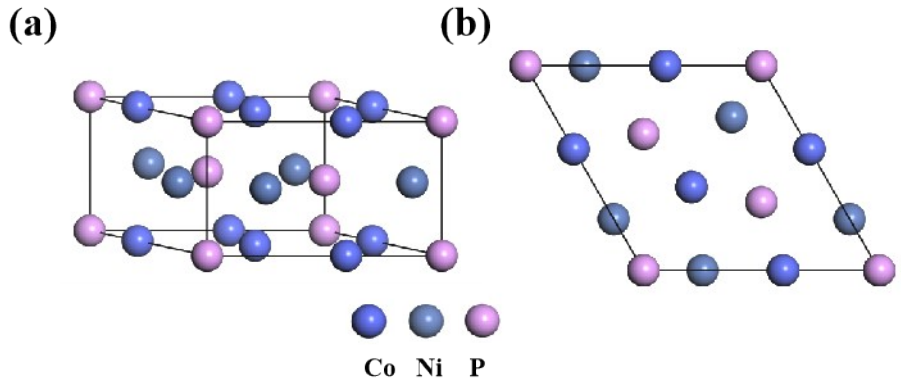

Figure S16. Bulk NiCoP: (a) side view and (b) top view.

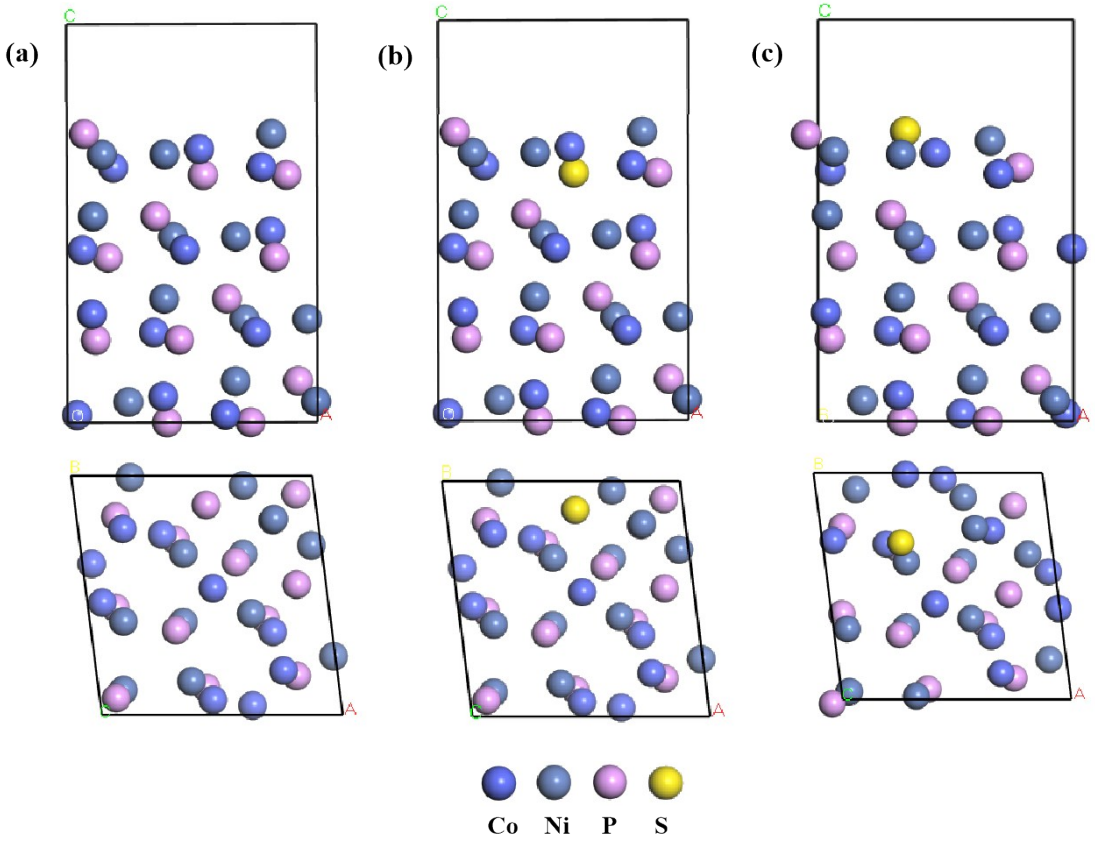

Figure S17. The (111) facet of (a) NiCoP, (b) S-NiCoP before structural optimization,

(c) S-NiCoP after structural optimization.

Table S1. The binding energy with H_2O* or H* adsorbed on different sites of S-NiCoP

Adsorbate	H_2O*		H*	
Site	Ni	Co	Ni	Co
Binding energy / eV	-240.690561	-240.815172	-229.1303221	-229.7176027

The d band center (ε_d) in Figure 4e can be calculated from the following formula:

$$\varepsilon_d = \frac{\int_{-\infty}^{\infty} x\rho(x)dx}{\int_{-\infty}^{\infty} \rho(x)dx}, \quad (11)$$

in which x and ρ(x) denote the energy (eV) and d-pdos of Co in Figure 4e.

Table S2. Comparison of HER performance of S-NiCoP with other electrocatalysts.

Catalyst	η_{10} / mV	η_{100} / mV	Electrolyte	References
S-NiCoP NW/CFP	102	170	1M KOH	This work
$Ni_{0.51}Co_{0.49}P$	82		1M KOH	Adv. Funct. Mater., 2016, 26, 7644-7651
NiCoP nanocone arrays/NF	104		1M KOH	J. Mater. Chem. A., 2017, 5, 14828-14837
$(Co_{0.52}Fe_{0.48})_2P$	79		1M KOH	Energy Environ. Sci, 2016, 9, 2257
Ni_5P_4 nanocrystals	118		0.5M H_2SO_4	J. Mater. Chem. A., 2015, 3, 1656
CoP/CC	67	204	0.5M H_2SO_4	J. Am. Chem. Soc., 2014, 136, 7587
Ni_2P-NiCoP/NCCs	116		1.0 M NaOH	J. Mater. Chem. A., 2017, 32, 16568-16572
S-CoP/NF	109	185	1M KOH	Nano Energy, 2018, 53, 286-295
Ni-modied CoP NPs	180		1M KOH	J. Mater. Chem. A., 2016, 20, 7549-7554
CoP NPs	170		1M KOH	Nano Energy, 2016, 29, 37-45
CoP/RGO	200		1M KOH	Chem. Sci., 2016, 7, 1690-1695
O-NiCoP	44		1M KOH	Small, 2018, 14, 1613-6829
$NiCo_2P_x$/CF	58	127	1M KOH	Advanced Materials, 2017, 29,1605502
S−Ni_5P_4 NPA/CP	56	104	0.5M H_2SO_4	ACS Appl Mater Interfaces, 2018, 10, 26303-26311
Ni_2P-Co_2P/NC	251		1M KOH	Inter. J. Hydrogen Energy, 2019, 44, 14908-14917
V-CoP/CC	71		1M KOH	Chem. Sci., 2018, 9, 1970-1975
	123		1M PBS	
	47		0.5M H2SO4	
NiCoP–C(TPA)/NF	78	~175	1M KOH	Catalysis Science & Technology, 2019, 9, 4651-4658.
	94		0.5M H_2SO_4	
	248		1M PBS	

REFERENCES

1. R. Zhang, X. Wang, S. Yu, T. Wen, X. Zhu, F. Yang, X. Sun, X. Wang and W. Hu, *Advanced materials*, 2017, **29**.

2. H. Liang, A. N. Gandi, D. H. Anjum, X. Wang, U. Schwingenschlogl and H. N. Alshareef, *Nano letters*, 2016, **16**, 7718-7725.
3. M. Caban-Acevedo, M. L. Stone, J. R. Schmidt, J. G. Thomas, Q. Ding, H. C. Chang, M. L. Tsai, J. H. He and S. Jin, *Nature materials*, 2015, **14**, 1245-1251.